High-Power-Factor Boost Rectifier with a Passive Energy Recovery Snubber

Marn-Go Kim and Seung-Ho Baek

Department of Control and Instrument. Eng., Pukyong National University
Yong-dang-dong 100, Nam-ku, Pusan 608-739, Korea
Tel: 051-620-1637, Fax: 051-623-4227

Abstract - A passive energy recovery snubber for high-power-factor boost rectifier, in which the main switch is implemented with a MOSFET, is described in terms of the equivalent circuits that are operational during turn-on and turn-off sequences. These equivalent circuits are analyzed so that the overshoot voltage across the main switch, the snubber current, and the turn-off transition time can be predicted analytically.

The main switch combined with proposed snubber can be turned on with zero current and turned off at limited voltage stress. The high-power-factor boost rectifier with proposed snubber is implemented, and the experimental results are presented to confirm the validity of proposed snubber.

I. Introduction

Snubbers are required to limit di/dt and dv/dt in the power semiconductor device, keep the device within its safe operating areas, and to reduce the switching power losses in the device. Conventional snubbers, which discharge via resistors, are simple to design and use, but the energy dissipated in the resistors is proportional to the switching frequency. Therefore, resistive snubbers are not practical at the high switching frequencies encountered in the modern power electronics system. In high frequency applications, it is necessary to use an energy recovery snubber to keep losses to a minimum, by regenerating the energy trapped in the snubber circuit back into the DC rail.

For the pulse-width-modulated(PWM) boost converter, several methods have been described to recover the trapped energy in the snubber circuit [1]-[4]. An active auxiliary switch is used in [1]-[2] to regenerate the trapped energy to DC output. The auxiliary switch also provides a soft switching for the main semiconductor switch. But, an additional control circuit is needed to drive the auxiliary switch. In [3], the trapped energy is transferred into the load through a DC/DC converter. This method could be expensive due to the energy recovery converter, as well as being more complex than other methods. A transformer may also be used as a passive element in an energy recovery circuit[4]. The turn-on snubber inductor is replaced with a transformer, so that the energy in the inductor is recovered into the output via the secondary winding of the transformer. The control circuit of this method is the same as that of the basic boost converter. However, the transformer for this snubber may be difficult to construct and the voltage on the main switching device may exceed the output voltage.

In this paper, a new energy recovery snubber which uses a few passive components is proposed for boost converter, and the operation principles and characteristics of the energy recovery snubber are presented. The validity of this snubber is verified through experiment.

II. Energy Recovery Snubber for Boost Converter

In a boost converter, the output voltage is greater than the input voltage. A basic boost converter is shown in Fig. 1. When Q is closed, the inductor current rises and energy is stored in the inductor L. The input current flows through inductor L and transistor Q. If the switch Q is opened, the energy stored in the inductor is transferred to load through diode D, and the inductor current falls. The input current would now flow through L, C, load, and diode D. Now, if the switch Q is turned on again, the diode D would behave as a short circuit. The rate of rise of the forward current of Q and the rate of fall of the forward current of D would be very high, tending to be infinity. The peak reverse current could be very high, and the power semiconductor devices may be damaged. This problem is normally overcome by connecting a di/dt limiting inductor, Ls, between Q and D. Unfortunately the di/dt limiting inductor is equally effective when the transistor is turned off and turns the diode D on again. A turn-off snubber is therefore needed to limit the rise of voltage across Q. If the switch Q is constructed with power MOSFETs, the switching speed of these devices is such that often no turn-off snubber is needed. Instead, a voltage limiter is used to absorb the rate of rise of the voltage across the MOSFETs [2]-[5].

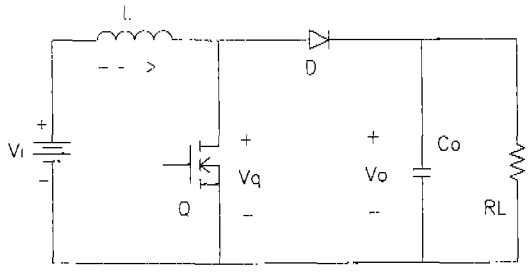

Fig. 1. Basic boost converter circuit.

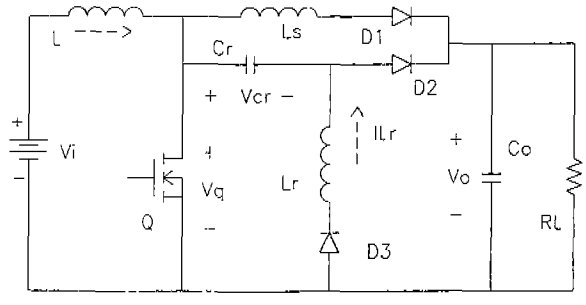

Fig. 2. Proposed boost converter circuit.

Fig. 2 shows the circuit diagram of proposed energy recovery snubber circuit for boost converter. Since the circuit uses power MOSFET, the purpose of turn-off snubber consisting of Cr and D2 is to clamp the voltage across this MOSFET. When Q is turned on, the rate of rise of the forward current of Q is limited by the current limiting inductor Ls. When Q is turned off, the flow of current to the load is gradually changed from D2 to D1, and the snubber capacitor Cr is charged to its positive peak value. If Q is turned on again, the trapped energy in Cr is discharged through D3 and Lr, and the polarity of the capacitor energy is reversed. During the next turn-off transition period of Q, the snubber energy is recovered into the load through Cr-D2 path or D3-Lr-D2 path.

III. Operation Analysis of Boost Converter with Proposed Snubber

To simplify the analysis, the following assumptions are made :

1) input filter inductance is large so that I_L is constant,

2) output filter capacitance is large so that Vo is constant,

3) all semiconductor devices are ideal.

Furthermore, the following symbols are also defined :

$w_1 = 1/\sqrt{L_s C_r}$, $Z_1 = \sqrt{L_s/C_r}$,

T_{on} = turn-on period of Q, $w_2 = 1/\sqrt{L_r C_r}$,

$Z_2 = \sqrt{L_r/C_r}$.

Depending on the operating conditions, the proposed snubber circuit can be in Region-1 operation in which the variation of $w_2 T_{on}$ is in the range from π to infinity, or in Region-2

opearation in which the variation of $w_2 T_{on}$ is in the range between 0 and π. The theoretical waveforms of Fig. 2 for Region 1 and 2 are shown in Fig. 3 and Fig 4, respectively. The converter goes through different topological modes(M1, M2, ..., M7) in a steady-state cycle. The corresponding equivalent circuits of the converter in each of the topological modes are given in Fig. 5. Since the voltage across output capacitor and the current on input inductor are both constant, they are replaced by the dc sources Vo and I_L, respectively.

A. Region-1 Operation ($w_2 T_{on} > \pi$)

The sequence of topological modes in Region-1 operation are M1, M2, M3, M4, M5, and M6. This operation occurs for $w_2 T_{on} > \pi$.

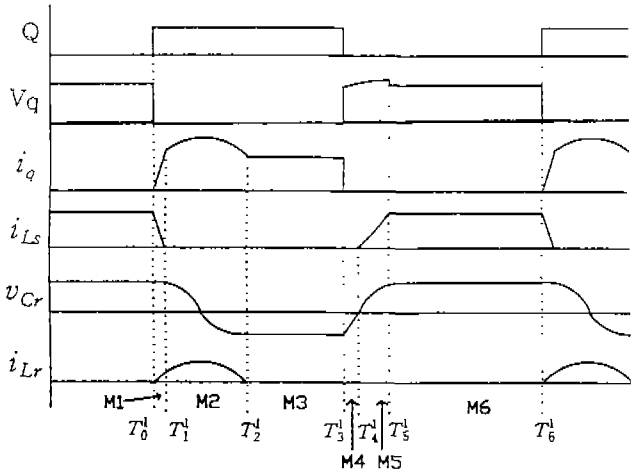

Fig. 3. Typical Region-1 waveforms.

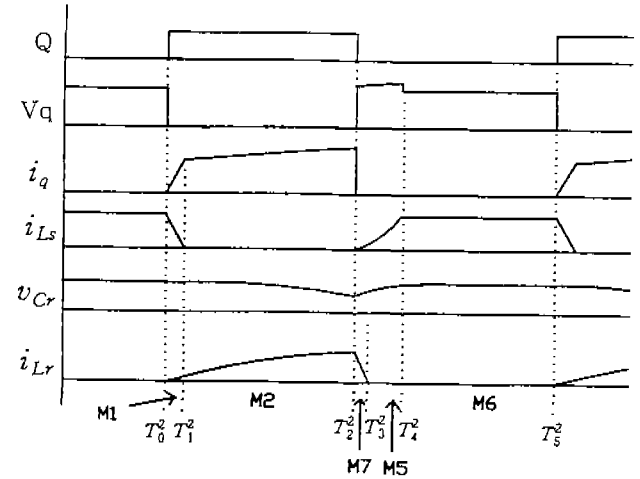

Fig. 4. Typical Region-2 waveforms.

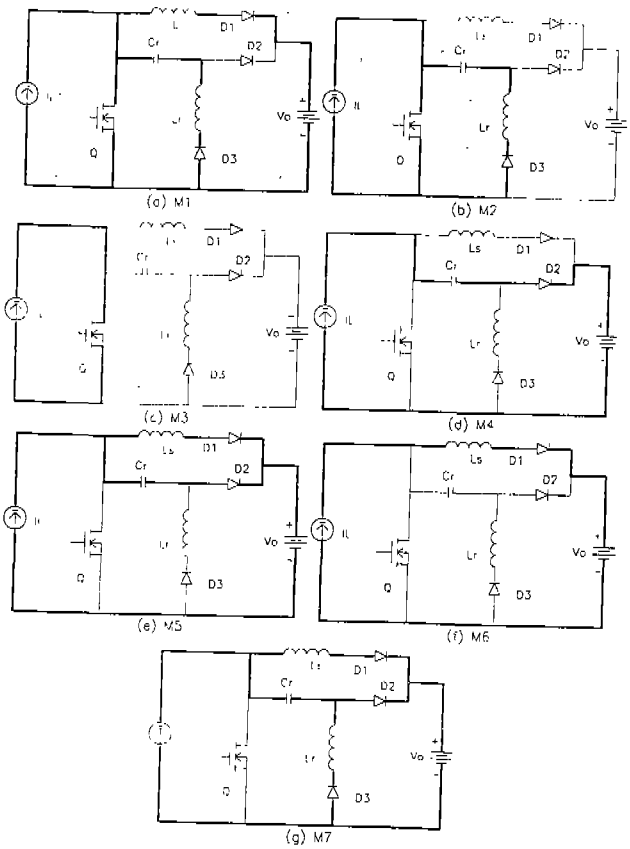

Fig. 5. Equivalent circuits for different topological modes.

a) $T_0^1 - T_1^1$ (M1) : Prior to T_0^1, the MOSFET Q is off, and the rectifier diode D1 is conducting. At T_0^1, Q is turned on. The Ls current linearly falls until it reaches 0, where D1 is turned off. The Lr current starts to increase due to the resonance between Lr and Cr Because of controlled di/dt at turn-on, the turn-on loss of Q is negligible and the peak reverse current of D1 can be limited.

b) $T_1^1 - T_2^1$ (M2) : Lr current continues to make a resonance until the resonance brings its current to zero at T_2^1. Cr voltage is decreased until its voltge becomes reversed peak value.

Using the initial Cr voltage of V_p and Lr current of zero at T_0^1, the resonant current and the resonant voltage equations during M1 and M2 can be written as

$$i_{Lr}(t) = V_p / Z_2 \sin w_2 t$$

$$v_{Cr}(t) = V_p \cos w_2 t \quad (1)$$

c) $T_2^1 - T_3^1$ (M3) : D3 is turned off at T_2^1. The operation of the circuit of this stage is identical to that of the basic boost converter.

d) $T_3^1 - T_4^1$ (M4) : At T_3^1, Q is turned off. Cr is linearly charged by I_L to zero voltage. The energy trapped in Cr is transferred into the load during this mode.

e) $T_4^1 - T_5^1$ (M5) : When the capacitor Cr voltage becomes zero, diode D1 is turned on. The voltage across Q is limited by $V_o + V_{Cr}$. The Ls current builds up and the charging current into Cr goes down to zero. The induced voltage on Ls is absorbed in the snubber capacitor Cr. This stage finishes when the Ls current becomes I_L and Cr voltage is charged to its peak value at T_5^1. The stress energy charge into Cr and the energy recovery into the load occur simultaneously during this mode.

Considering that the initial Ls current and Cr voltage are zeros at T_4^1, the state equations during M5 are given :

$$i_{Ls}(t) = I_L(1 - \cos w_1 t)$$
$$v_{Cr}(t) = Z_1 I_L \sin w_1 t \,. \quad (2)$$

f) $T_5^1 - T_6^1$ (M6) : This interval is identical to the freewheeling stage of the basic boost converter. During this stage, energy transfer from source to load occurs. At T_0^1, Q is turned on again, starting another switching cycle.

B. Region-2 Operation($0 < w_2 T_{on} \leq \pi$)

The sequence of topological modes in Region-2 operation are M1, M2, M7, M5, and M6. M1 and M6 of Region-2 operation are similiar to those of Region-1 operation.

a) $T_1^2 - T_2^2$ (M2) : Lr current continues to make a resonance until Q is turned off. The Cr voltage is reduced to negative value at T2 when $w_2 T_{on}$ varies from $\pi/2$ to π. For $0 < w_2 T_{on} \leq \pi/2$, the Cr voltage is reduced to positive value at T_2^2.

For the interval $T_0^2 - T_2^2$, the state equations of LrCr tank in Region-2 operation can be expressed as (1) of Region-1 operation.

b) $T_2^2 - T_3^2$ (M7) : At T_2^2, Q is turned off, and its voltage is limited by Vo+ V_{Cr} due to the conduction of D2. The energy stored in the inductor Lr is directly transferred into the load. Lr current goes down to zero at T_3^2. The input current goes into the load through Ls-D1 or Cr-D2. For $\pi/2 < w_2 T_{on} \leq \pi$, the input current flowes entirely via Cr-D2 path until the Cr voltage is charged by I_L to zero. When the value of Cr voltage is greater than zero, D1 is turned on.

c) $T_3^2 - T_4^2$ (M5) : The Ls current builds up until it reaches I_L at T_4^2. The charging current into Cr gradually goes down to zero.

During the conduction of both D1 and D2, the Ls current and the Cr voltage can be expressed as the following :

$$i_{Ls} = V_{Cr}(0)/Z_1 \sin w_1 t + I_L(1 - \cos w_1 t)$$
$$v_{Cr}(t) = V_{Cr}(0) \cos w_1 t + Z_1 I_L \sin w_1 t \quad (3)$$

where the initial Ls current is zero and $V_{Cr}(0)$ is the Cr voltage at the start of D1 conduction. Since $V_{Cr}(0)$ is not less than zero, $V_{Cr}(0)$ can be derived from (1) as

$$V_{Cr}(0) = 0, \text{ for } \pi/2 < w_2 T_{on} \leq \pi \quad \text{and}$$
$$V_{Cr}(0) = V_p \cos w_2 T_{on}, \text{ for } 0 < w_2 T_{on} \leq \pi/2. \quad (4)$$

When $w_2 T_{on}$ varies from $\pi/2$ to π, the equation (3) is equal to (2). Using (3), the Lr current and the peak capacitor voltage V_p at the end of M5 can be derived as

$$I_L = V_{Cr}(0)/Z_1 \sin w_1 t_{off} + I_L(1 - \cos w_1 t_{off})$$
$$V_p = V_{Cr}(0) \cos w_1 t_{off} + Z_1 I_L \sin w_1 t_{off} \quad (5)$$

where t_{off} is the transition time of Ls current from 0 to I_L for $0 < w_2 T_{on} \leq \pi/2$.

IV. Operation Characteristics

A Overshoot voltage across Q

When Q is turned off, it experiences a voltage in excess of the output voltage due to the induced voltage across Ls. Ls current builds up until it reaches the input current I_L at the end of M5. At this point, the Cr voltage is charged to a peak value V_p .

From (2) and (3), the overshoot voltage V_p can be derived as follows :

$$V_p = Z_1 \cdot I_L, \text{ for } \pi/2 < w_2 T_{on} \text{ and}$$

$$V_p = \frac{Z_1 \cdot I_L}{\sin w_2 T_{on}}, \text{ for } 0 < w_2 T_{on} \leq \pi/2. \quad (6)$$

The overshoot voltage is normalized with respect to $Z_1 \cdot I_L$, and the normalized voltage is plotted in Fig. 6. The normalized overshoot voltage across the main switch is reduced to 1 as $w_2 T_{on}$ varies from zero to $\pi/2$, and then it is fixed at 1 for $w_2 T_{on} > \pi/2$.

B. Peak Lr current

When Q is turned on, apart from taking of the input current, it also sees the Lr current and the diode reverse recovery current. The Lr current reaches a peak value during M2.

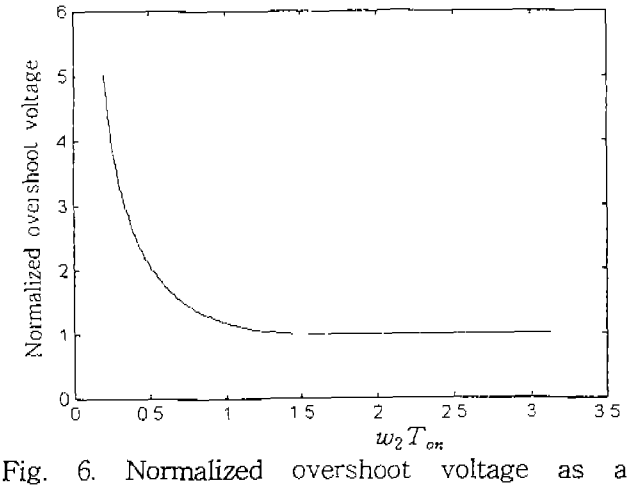

Fig. 6. Normalized overshoot voltage as a function of $w_2 T_{on}$.

From (1), the peak Lr current I_p can be expressed as

$$I_p = V_p/Z_2, \text{ for } \pi/2 < w_2 T_{on} \text{ and}$$

$$I_p = V_p/Z_2 \sin w_2 T_{on}, \text{ for } 0 < w_2 T_{on} \leq \pi/2. \quad (7)$$

Substituting (6) into (7) gives

$$I_p = Z_1 \cdot I_L/Z_2 = \sqrt{Ls/Lr} \cdot I_L . \quad (8)$$

The peak Lr current is directly proportional to the input current. The proportional coefficient is determined by the square root of ratio of the current limiting turn-on inductor Ls to the resonant tank inductor Lr.

C Turn-off transition time

When Q is turned off, the input current flows into the load through Cr-D2 or Ls-D1 path. When Cr voltage is negative, which may occur for $w_2 T_{on} > \pi/2$, the current goes entirely via Cr-D2 path When Cr is charged by I_L to zero, D1 is turned on Then, Lr current builds up until it reaches I_L. When Lr current is equal to I_L , the turn-off transition is ended.

a) $\pi/2 < w_2 T_{on}$

From the voltage equations of (1) and (6), the Cr voltage at the end of conduction period of Q can be written as

$$V_{Cr}(T_{on}) = Z_1 \cdot I_L \cos w_2 T_{on} \text{ for } \pi/2 < w_2 T_{on} < \pi$$

$$\text{and } V_{Cr}(T_{on}) = -Z_1 \cdot I_L \text{ for } \pi < w_2 T_{on}. \quad (9)$$

Using (9), the charging time of Cr by I_L to zero when Q is turned off can be derived as

$$t_c = -1/w_1 \cos w_2 T_{on}, \text{ for } \pi/2 < w_2 T_{on} \leq \pi$$

$$\text{and } t_c = 1/w_1 , \text{ for } \pi < w_2 T_{on} \quad (10)$$

From (2), the transition time for changing the flow of input current from Cr-D2 to Ls-D1 is $\pi/(2w_1)$. Therefore, the total turn-off transition time t_{off} , which is the time interval of $T_3^1 - T_5^1$

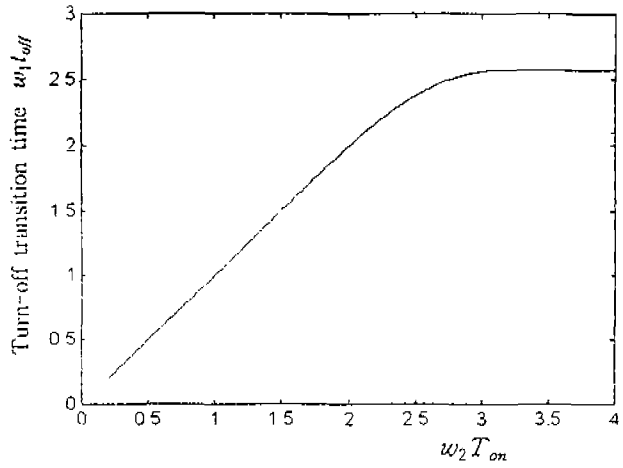

Fig. 7. Turn-off transition time as a function of w_2T_{on}

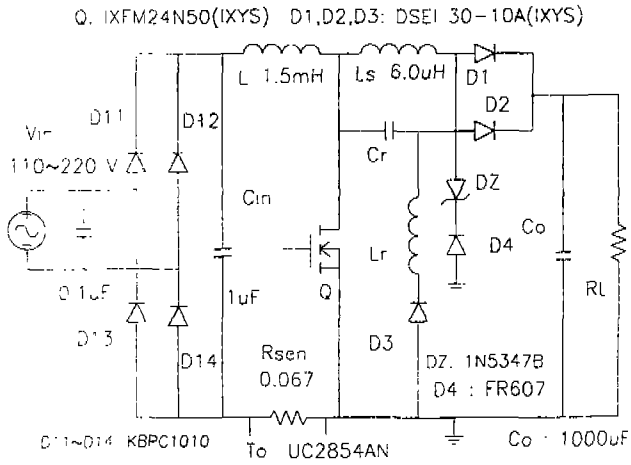

Fig. 8. Experimental boost rectifier circuit.

for the typical Region-1 waveform of Fig. 3 and $T_2^2 - T_4^2$ for the typical Region-2 waveform of Fig. 4, can be expressed as

$$w_1t_{off} = -\cos w_2T_{on} + \pi/2, \text{ for } \pi/2 < w_2T_{on} \leq \pi$$

and $w_1t_{off} = 1 + \pi/2$, for $\pi < w_2T_{on}$. (11)

b) $0 < w_2T_{on} < \pi/2$

When Q is turned off, D1 is turned immediately on. From (4) and (6), the initial Cr voltage can be derived as

$$V_{Cr}(0) = Z_1 \cdot I_L / \tan w_2T_{on} \quad (12)$$

Substituting (12) into the current equation of (5) gives

$$w_1t_{off} = w_2T_{on} \quad (13)$$

Using (11) and (13), the turn-off transition time w_1t_{off} is plotted as a function of w_2T_{on} in Fig. 7. The turn-off transition time w_1t_{off} varies from 0 to 2.57, depending on w_2T_{on} .

V. Experimental Results

A 100-kHz, 500W high-power-factor boost rectifier with the proposed energy recovery snubber has been implemented to demonstrate the operation. It is regulated at 375-V output

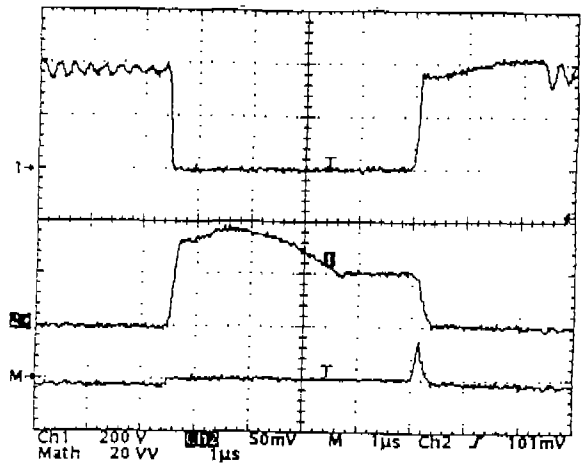

Fig. 9. Measured voltage(upper trace-200 V/div), current(middle trace-5 A/div), and loss(lower trace-2 kW/div) waveforms of Q operating in Region-1 (time scale: 1 μ s/div).

with a 110-220 VAC input range. The power stage circuit diagram is given in Fig. 8, which is implemented in conjunction with a control circuit [6]. The diodes Dz and D4 are used to limit the reverse voltage of D1 to Vo+VDz when Q is turned on. The main switch Q is implemented with a MOSFET.

Fig. 9 shows the measured voltage, current, and loss waveforms of Q operating in Region-1. The snubber components are chosen as : Ls = 6.0 μH, Cr = 0.1 μF, and Lr = 10 μH. It can be seen that the turn-on loss of the main

switch Q is negligible due to the action of the current limiting inductor Ls, and the turn-off loss of this switch is smaller compared to that of the conventional boost converter due to the reduced turn-off voltage stress of Q. As shown in the voltage waveform of this figure, the measured turn-off transition time t_{off} is about 2.2 μs, and the measured T_{on} is 4.4 μs. Since $w_2 T_{on}$ is 4.4, the theoretical t_{off} can be calculated from (11) as 2.0 μs. The small discrepancy between the measured and theoretical t_{off} is mainly due to both the nonideal switching devices and the existence of stray impedance parameters in the experimental circuit.

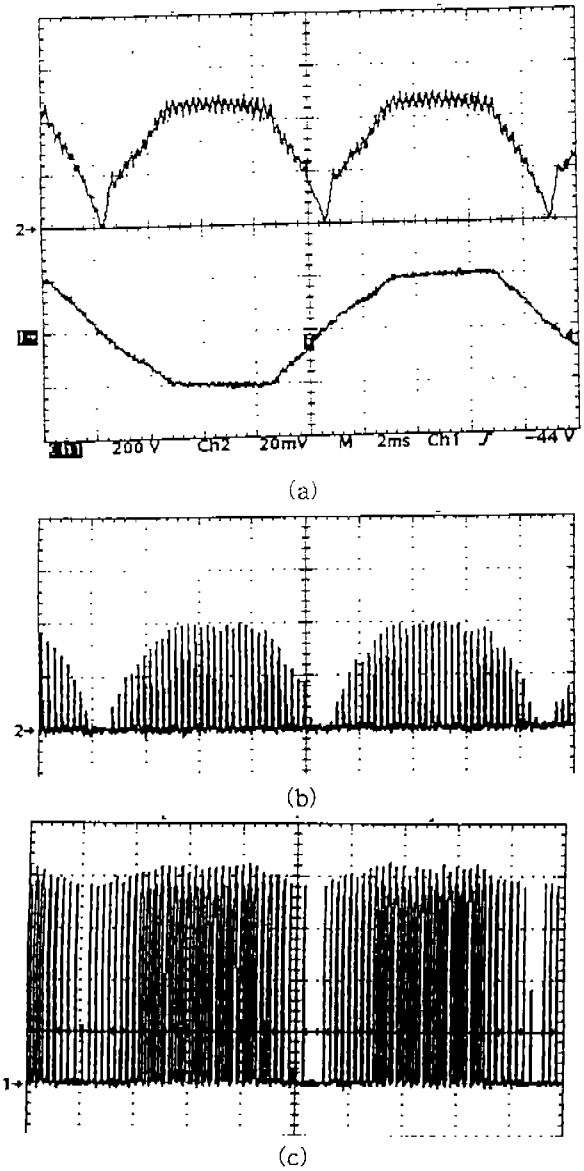

(a)

(b)

(c)

Fig. 10. Measured Region-1 boost converter waveforms (time scale: 2 ms/div). (a) I_L (2 A/div) and Vin(200 V/div), (b) Lr current (2 A/div), and (c) V_q (100 V/div).

Fig. 10 shows the measured Region-1 waveforms for the boost inductor current I_L, Lr current, and the voltage across Q at 120 Hz, which are presented together with the ac input voltage. In this figure, the peak input voltage is 200-V and the maximum I_L current is 5-A. Using (8), the theoretical maximum peak Lr current can be calculated as 3.87 A. The measured Lr current coincides quite well with the theoretical one. When the boost converter is operating at 200-V input voltage , the duty ratio of experimental boost converter is 0.467, and hence T_{on} is 4.67 μs. Using (6), the maximum overshoot voltage can be calculated as 38.7-V, and the theoretical maximum Vq becomes 413.7-V. Again, the agreement between measured and theoretical overshoot voltage is good.

Fig. 11 shows the measured voltage, current, and loss waveforms of Q operating in Region-2. The snubber components are chosen as : Ls = 6.0 μH, Cr = 0.47 μF, and Lr = 110 μH. It can be seen that the turn-on loss of Q is

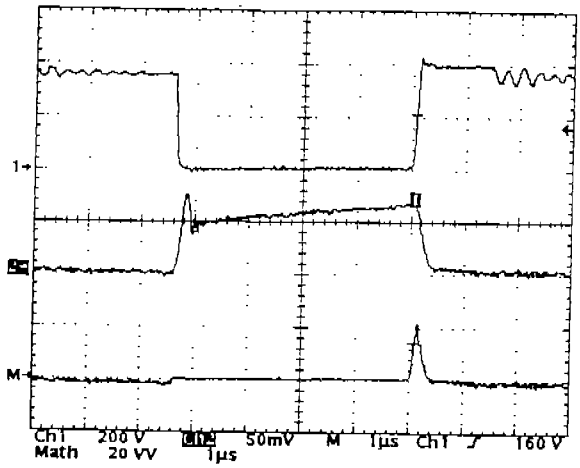

Fig. 11. Measured voltage(upper trace-200 V/div), current(middle trace-5 A/div), and loss(lower trace-2 kW/div) waveforms of Q operating in Region-2 (time scale: 1 μs/div).

negligible, but the turn-off loss is still significant due to high turn-off current. The turn-off current of Q can be reduced to I_L if the snubber is designed to be operated in Region-1. As shown in the voltage waveform of this figure, the measured turn-off transition time t_{off} is about 1.2 μs, and the measured T_{on} is 4.4 μs. Since $w_2 T_{on}$ is 0.61, the theoretical t_{off} can be calculated from (13) as 1.03 μs.

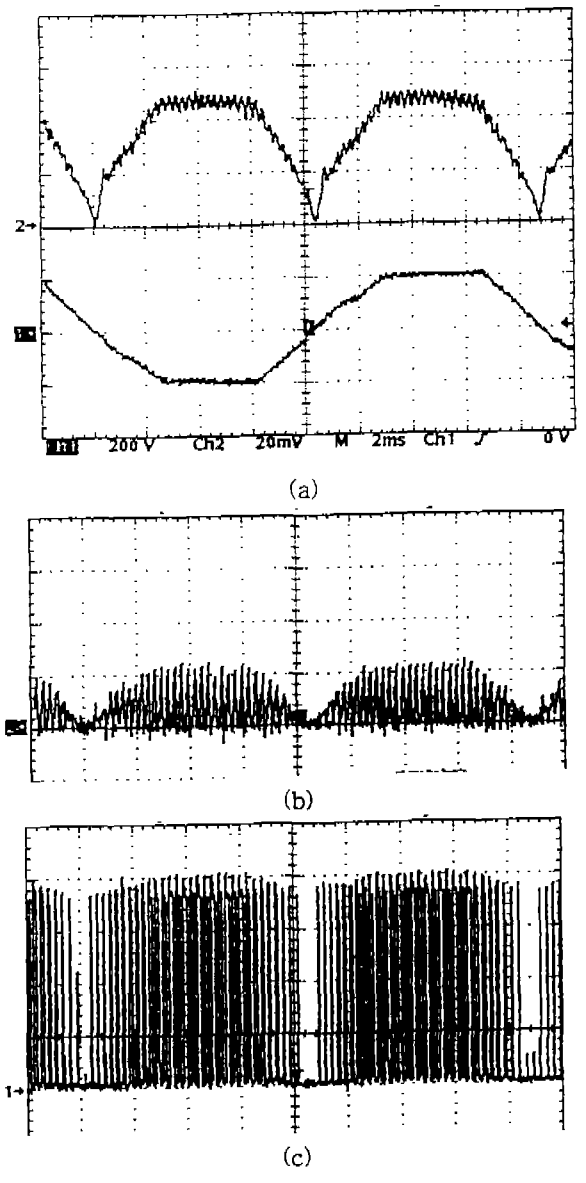

Fig. 12. Measured Region-2 boost converter waveforms (time scale: 2 ms/div). (a) I_L (2 A/div) and Vin(200 V/div), (b) Lr current (1 A/div), and (c) V_q (100 V/div).

Fig. 12 shows the measured Region-2 waveforms for the boost inductor current I_L, Lr current, and the voltage across Q at 120 Hz, which are also presented together with the ac input voltage. In this figure, the peak input voltage is 200-V and the maximum I_L current is 5-A. Using (8), the theoretical maximum peak Lr current can be calculated as 1.17 A. The measured Lr current coincides quite well with the theoretical one. When the boost converter is operating at 200-V input voltage , the duty ratio of experimental boost converter is 0.467, and hence T_{on} is 4.67 μs. Using (6), the maximum overshoot voltage can be calculated as 29.6-V, and the maximum Vq becomes 404.6-V. The agreement between measured and theoretical overshoot voltage is good.

The input ac voltage and current for both Region-1 and Region-2, which demonstrates the high power factor of proposed boost rectifier, are shown in Fig. 13. The measured efficiency of the implemented converter shows 97.5 % at high-line-input voltage and 94.5 % at low-line-input voltage in Region-1 operation. The efficiency for Region-2 operation is measured as 96.5 % at high-line-input voltage and 91.5 % at low-line-input voltage. The

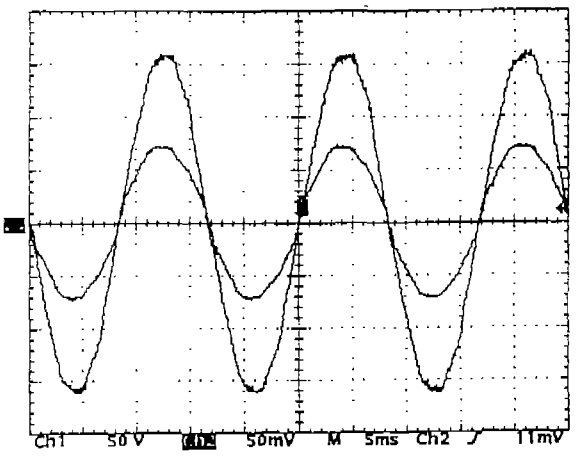

Fig. 13. Measured input voltage (outer trace-50 V/div) and current (inner trace-5 A/div) waveforms(time scale: 5 ms/div).

measured efficiency of boost rectifier operating in Region-1 is 1-3% higher than that of the rectifier operating in Region-2. The measured power factor is 0.99.

If Q is an IGBT, the reduction of turn-off loss should be needed. When the proposed snubber is combined with the passive recovery snubber [7], the turn-off loss could be minimised by controlling the voltage trajectory across the main switch from zero to clamp voltage.

VI. Conclusion

A passive energy recovery snubber for boost converter has been presented. The main switch Q of the boost converter, which is implemented with a MOSFET in this paper, is turned on with zero current and turned off with a limited voltage clamp. When the snubber is designed to be operated in Region-1, the turn-on loss of Q is negligible and the turn-off loss of the switch becomes smaller compared to that of the conventional boost converter. In Region-2 operation of the snubber, the turn-on loss of Q is negligible, but the turn-off loss of the switch is still significant due to high turn-off current. If the main switch is constructed with an IGBT, the passive recovery snubber [7] can be added to the proposed snubber to control the rate of rise of its voltage from zero to the voltage clamp, and to reduce the turn-off loss to a minimum.

The operation analysis for the proposed snubber has been done. The overshoot voltage across the main switch is derived and normalized with respect to $Z_1 I_L$. The normalized overshoot voltage is reduced to 1 as $w_2 T_{on}$ varies from zero to $\pi/2$, and then it is fixed at 1 for $w_2 T_{on} > \pi/2$. The peak snubber inductor current is directly proportional to the input current. The proportional coefficient is determined by the square root of ratio of the current limiting turn-on inductor Ls to the resonant tank inductor Lr. The turn-off transition time $w_1 t_{off}$ varies from 0 to 2.57, depending on $w_2 T_{on}$.

The high-power-factor boost rectifier with a passive energy recovery snubber is implemented to confirm the operation. The experimental results show good agreement with the theoretical ones The measured efficiency of the boost rectifier operating in Region-1 is 1-3% higher than that of the rectifier operating in Region-2. The measured power factor is 0.99.

References

[1] K. Chen, A Elasser, and D.A. Torrey, " A soft switching active snubber optimized for IGBTs in single switch unity power factor three phase diode rectifiers, " IEEE Trans Power Electron , vol. 10, no. 4, pp. 446-452, July 1995.

[2] G.C. Hua, C.S. Leu and F.C. Lee, " Novel zero-voltage-transition PWM converter, " IEEE PESC Record, pp 55-61, 1992

[3] N. Backman and H. Thorsland, " A new light-weight 100A/48V three phase rectifier, " IEEE Intelec91 Record, pp. 92-97,1991.

[4] G. Cali, " Harmonic distortion reduction schemes for a new 100A-48V power supply, " IEEE Intelec92 Record, pp. 524-531, 1992

[5] J.G. Kassakian, M.F. Schlecht, and G.C. Verghese, Principles of Power Electronics. Reading, MA: Addison-Wesley, 1991, chap. 24.

[6] L. Dixon, " High power factor switching preregulator design optimization," Unitrode power design seminar, 1991.

[7] S.J. Finney, B.W. Williams, and T.C. Green, " RCD snubber Revisited, " IEEE Trans. Ind. Applicat., vol. 32, no. 1, pp. 155-160, January/February 1996.